AD-A099 294 MATERIALS RESEARCH LABS ASCOT VALE (AUSTRALIA) F/G 11/6
INFLUENCE OF REMELTING CONDITIONS ON THE PERFORMANCE OF LOW ALL--ETC(U)
OCT 80 R C ANDREW, G M WESTON, G CLARK
UNCLASSIFIED MRL-R-786 NL

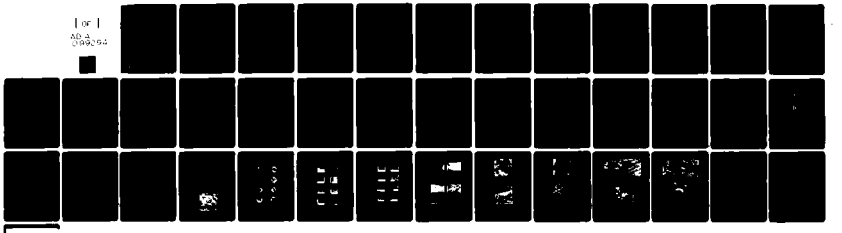

END
DATE FILMED
6-81
DTIC

MRL-R-786

(12)

AR-002-364

DEPARTMENT OF DEFENCE

DEFENCE SCIENCE AND TECHNOLOGY ORGANISATION

MATERIALS RESEARCH LABORATORIES

MELBOURNE, VICTORIA

REPORT

MRL-R-786

INFLUENCE OF REMELTING CONDITIONS ON THE PERFORMANCE OF LOW ALLOY ESR STEEL IN THE AS-CAST CONDITION - SMALL LABORATORY INGOTS

Richard C. Andrew, George M. Weston and Graham Clark

Approved for Public Release

OCTOBER, 1980

DEPARTMENT OF DEFENCE

MATERIALS RESEARCH LABORATORIES

REPORT

MRL-R-786

INFLUENCE OF REMELTING CONDITIONS ON THE PERFORMANCE OF LOW ALLOY ESR STEEL IN THE AS-CAST CONDITION - SMALL LABORATORY INGOTS

Richard C. Andrew, George M. Weston and Graham Clark

ABSTRACT

The mechanical properties of three ingots of a low-alloy steel produced in an experimental ESR furnace are assessed in the as-cast, heat-treated condition. In general, the tensile, notch impact toughness, fracture toughness and fatigue properties of these ingots compare favourably with those determined for a wrought, vacuum-degassed electric furnace steel of similar composition. Variations in mechanical properties within, as well as between, ingots are correlated with differences in chemical composition, inclusion content, inclusion morphology and solidification geometry brought about by changes in the remelting conditions.

Approved for Public Release

POSTAL ADDRESS: Chief Superintendent, Materials Research Laboratories
P.O. Box 50, Ascot Vale, Victoria 3032, Australia

DOCUMENT CONTROL DATA SHEET

Security classification of this page: UNCLASSIFIED

1. DOCUMENT NUMBERS:
   a. AR Number: AR-002-364
   b. Series & Number: REPORT MRL-R-786
   c. Report Number: MRL-R-786

2 SECURITY CLASSIFICATION:
   a. Complete document: UNCLASSIFIED
   b. Title in isolation: UNCLASSIFIED
   c. Abstract in isolation: UNCLASSIFIED

3. TITLE:
INFLUENCE OF REMELTING CONDITIONS ON THE PERFORMANCE OF LOW ALLOY ESR STEEL IN THE AS-CAST CONDITION - SMALL LABORATORY INGOTS

4. PERSONAL AUTHOR(S):
ANDREW, Richard C.,
WESTON, George M. and
CLARK, Graham

5. DOCUMENT DATE: OCTOBER, 1980

6. TYPE OF REPORT & PERIOD COVERED:

7. CORPORATE AUTHOR(S):
Materials Research Laboratories

8. REFERENCE NUMBERS:
   a. Task: DST 77/062
   b. Sponsoring Agency:

9. COST CODE: 544840

10. IMPRINT (Publishing establishment)
Materials Research Laboratories
P.O. Box 50, Ascot Vale, Vic. 3032

OCTOBER, 1980

11. COMPUTER PROGRAMME(S):
(Title(s) and language(s)):

12 RELEASE LIMITATIONS (of the document):

Approved for Public Release

12 O. OVERSEAS: N C | | P R | 1 | A | | B | | C | | D | | E | |

13. ANNOUNCEMENT LIMITATIONS (of the information on this page)

No Limitation

14. DESCRIPTORS:

630 Low Alloy Steels
625 Electroslag Refined Steels

15 COSATI CODES: 1106 1308

16. ABSTRACT (if this is security classified the announcement of this report will be similarly classified)

The mechanical properties of three ingots of a low-alloy steel produced in an experimental ESR furnace are assessed in the as-cast, heat-treated condition. In general, the tensile, notch impact toughness, fracture toughness and fatigue properties of these ingots compare favourably with those determined for a wrought, vacuum-degassed electric furnace steel of similar composition. Variations in mechanical properties within, as well as between, ingots are correlated with differences in chemical composition, inclusion content, inclusion morphology and solidification geometry brought about by changes in the remelting conditions.

CONTENTS

INFLUENCE OF REMELTING CONDITIONS ON THE PERFORMANCE OF LOW ALLOY ESR STEEL IN THE AS-CAST CONDITION - SMALL LABORATORY INGOTS

1. INTRODUCTION

While casting technology has steadily improved to the stage where it is now possible to make small steel castings which can compete with forgings in terms of cost and performance, castings generally continue to be at a disadvantage when comparison of mechanical properties are made with wrought material of similar composition. Although high strengths can be obtained in steel castings by suitable heat-treatment, their ductility and toughness are often variable and low.

The main factors responsible for the inferior properties of castings are unsoundness, inhomogeneity, and non-metallic inclusions. The first two factors result from limitations in control over the solidification conditions which prevail in conventional casting processes whilst the third is primarily determined by the purity of the solidifying metal. Any improvement in the integrity of castings to make them more competitive with forgings depends upon control of these factors. Careful scrap selection, controlled de-oxidation, and vacuum melting or degassing all contribute to the delivery to the mould cavity of liquid with low inclusion-forming potential. However, control of the solidification conditions to enable the formation of a sound, homogeneous casting is more difficult.

One process which shows potential for the production of cast material of high integrity is electroslag-refining (ESR). The recent rapid acceptance of this process as a major supplier of premium-quality steel ingots to the forging industry is based upon the fact that both the remelting environment and the solidification parameters can be closely controlled.

1.1 Description and Benefits of the ESR Process

1.1.1 Structural Refinement

The process has been described in detail by several authors [1-3]. In essence, a consumable electrode of the desired composition is remelted

through a molten slag bath contained in a water-cooled copper mould (Fig. 1). This electrode forms one pole of an electrical circuit with the slag bath acting as a resistance element. When sufficient current is passed through the circuit to raise the temperature of the slag bath above the melting point of the electrode, the electrode tip begins to melt. Droplets of molten metal then fall from the tip through the slag bath, collecting in the bottom of the mould where they solidify to form the desired ingot. The steady stream of droplets maintains a constant supply of super-heated liquid to the pool on the top of the ingot.

Progressive melting and re-solidification along the vertical axis of a water-cooled mould in this manner results not only in the volume of molten metal remaining relatively constant for the bulk of ingot formation but also in the volume of molten metal being considerably less than that present during conventional casting of an ingot of similar size. For example, it is estimated that the volume of molten metal in an 800 mm diameter by 3000 mm long conventional mould at the beginning of ingot solidification is about 50 times greater than that present at any one time in an ESR mould of similar dimensions.

Ingot quality is reported to benefit substantially from the ESR mode of ingot formation. For instance, solidification times and therefore micro-segregation distances are substantially reduced, [4] while micro-porosity is minimized [5]. Even in large ingots, macro-porosity and macro-segregation are virtually eliminated [6].

1.1.2 Chemical Refinement

In addition to the benefits in solidification, the ESR process also improves steel cleanness. Reactions between the molten metal and the slag bath may dramatically reduce the oxide and sulphide inclusion content of the remelted ingot [7,8]. Indeed, a major strength of the process has been its capacity to desulphurize the melt. The inclusions which do form in the re-melted ingot are, because of the shorter local solidification time and the vertical solidification pattern, smaller and more uniformly distributed than in conventionally-cast ingots [1,2]. As well, Allibert et al. [9] and Mitchell [10] have reported that inclusion composition may be changed by interaction with the slag components.

The two main reactions which control sulphur removal in the ESR process are a slag-metal reaction and a gas-slag reaction [1]:

Slag-metal reaction

$$[S] + (O^{2-}) \rightleftharpoons (S^{2-}) + [O] \qquad (1)$$

Gas-slag reaction

$$(S^{2-}) + \frac{3}{2}\{O_2\} \rightleftharpoons \{SO_2\} + (O^{2-}) \qquad (2)$$

where [ ], ( ) and { } refer to metal, slag and gas respectively. Thus, sulphur removal is promoted by high slag basicity and a high oxygen partial pressure in the furnace atmosphere. Marked sulphur removal may be obtained regularly when lime-rich slags are used in combination with moulds which are open to an air atmosphere. Some desulphurization may be achieved with

slags which nominally do not contain any basic oxides because pyrohydrolysis of CaF_2 during pre-fusion may lead to the formation of up to 5% CaO by the reaction [1]

$$CaF_2 + H_2O \rightleftharpoons CaO + 2HF \qquad (3)$$

Furnace atmosphere plays an important role in desulphurization. Provision of an inert atmosphere, such as argon, above the slag bath effectively halts sulphur removal once the slag becomes saturated with sulphur; the saturation level is determined by the sulphur capacity of the slag.

Another important reaction which may affect the inclusion level of the remelted ingot is

$$3[Si] + 2(Al_2O_3) \rightleftharpoons 3(SiO_2) + 4[Al] \qquad (4)$$

It has been demonstrated [9] that the aluminium and silicon levels of the ingot can be adjusted by manipulating slag composition in accordance with this reaction. The high-alumina, silicon-free slags in general commercial usage normally lead to an accumulation of Al in the metal. Duckworth and Hoyle [1] have noted that an increase in aluminium and oxygen levels can be expected after remelting when slags containing in excess of 5% Al_2O_3 are used.

1.2 As-cast Products

Although the major application of the ESR process is the production of premium quality forging ingots, a small but expanding interest is being shown in the use of ESR material in the as-cast and heat-treated condition. Numerous mechanical property evaluations have been performed on ESR material and generally a high level of values is obtained. These results suggest that cast ESR material may provide a shorter and more economical processing than forging for some components. Initially this interest was confined to the production of medium to large components of complex shape in near-finished shape. The principal supporter of the electroslag casting (ESC) process, as it has come to be known, has been the Paton Institute in the USSR [11]. Work there, and subsequently at the University of British Columbia [12], had demonstrated that not only can components of complex shape be formed but also that the mechanical properties of these castings are isotropic and are at least equivalent to those of their wrought conventionally-melted counterparts. The range of application of ESC components is potentially very large. Mitchell [13] has suggested that it can best be applied to sections of thickness between 50 and 1500 mm, and castings of weight between 50 and 50,000 kg. The ESC process is currently used routinely in the USSR and eastern Europe for the production of an extensive range of items including valve bodies, pressure vessel nozzles, gears, crank-shafts, hobbing cutters and rolls [11,13]. Applications of the ESC process outside these countries are limited, with the production of hollows being the most common application. Several variations of this specialised form of the ESC process have been developed to enable hollows to be produced in a range of sizes [14,16].

More recently, interest has been shown in the production of components of complex shape by machining them directly from as-cast ESR ingots of simple

shape (Fig. 1). For example, the Lukens Steel Company [17] is currently considering applications such as hydraulic turbine generator components, quadrant rollers for hot spinning equipment, and components of mud pumps for oil rigs.

1.3 Areas of Defence Interest

The higher performance coupled with greater reliability and uniformity of wrought ESR steel, reported for civilian applications, was responsible for the initial arousal of Defence interest in the process. Front-line Defence components, such as ordnance, are now routinely manufactured from wrought ESR steel whilst other applications are being closely studied. It is expected that a similar development pattern will ensue for as-cast and heat-treated ESR steel because of the cost advantages which may result for components such as gun barrels, breech rings, and breech blocks.

Some information has been published on the performance of as-cast ESR steel of gun barrel compositions. Underwood [18] has reported similar fracture toughness values for wrought ESR and as-cast ESR Ni-Cr-Mo steel over the range of yield stress from 850 to 1200 MPa. In another example, an experimental 81 mm mortar barrel made in Israel from as-cast ESR steel has withstood firing tests with charges up to 143% of normal [5]. In fact, the mechanical properties of this as-cast and heat-treated steel satisfied the mechanical property specification for forged gun barrels.

In general, however, there is a paucity of information on the performance of as-cast and heat-treated low-alloy ESR steels, particularly in regard to structure-sensitive properties such as fracture toughness and resistance to fatigue crack propagation. These properties play an important part in determining the life of high performance gun barrels. Furthermore, information is also lacking on the processing history of those materials which have been evaluated and reported in the literature. This information is essential because factors such as electrode processing route, slag composition, deoxidation practice, furnace size and type, as well as operating conditions (voltage, melt rate, etc.), all influence the quality of the remelted ingot. A recent overseas visit by one of the authors (RCA) established that comparisons between the properties of ESR steel and those of steel from other processing routes could be invalid because of the failure to take fully into account these processing details.

1.4 Purpose of the Present Work

The purpose of the work described in this report has been to evaluate the performance of as-cast and heat-treated low alloy ESR steels using a range of mechanical testing procedures, and to assess the influence of remelting conditions on this performance. Initially, the properties of small ingots produced at MRL using the d.c. power mode have been determined; these results are covered by the present report. It is planned to extend the work to include both the a.c. power mode and larger ingot sizes when the furnace capacity is upgraded. In addition, samples of as-cast low-alloy ESR steel in ingot sizes up to 800 mm dia. are being sought from several commercial sources for inclusion in this evaluation programme.

2. EXPERIMENTAL

Ingots designated 42, 43 and 44 were produced for mechanical property evaluation in the experimental ESR furnace at MRL [19] using the d.c. electrode negative power mode*. Details of the remelting conditions for each ingot are summarised in Table I.

Two mould sizes, nominally 70 and 100 mm diameter, were used to enable the effect of ingot diameter on performance to be assessed. Small diameter ingots are regularly produced overseas without deoxidation procedures [26]. Vaporised slag components and slag reaction products are allowed to accumulate in the mould, thereby preventing the ingress of oxygen to the slag bath. In view of this, deoxidants were not added to the slag bath during the remelting of the three ingots. As an added precaution, argon was bled into the mould cavity during the remelting of ingot 43. The surface of the electrodes, which were commercial grade En25 steel, were ground prior to remelting to eliminate a potential source of FeO in the slag bath. To obtain ingots with a range of sulphur and inclusion levels, two slags with different desulphurizing capacities were used, nominally 90% CaF_2 + 10% Al_2O_3 and 33% CaF_2 + 33% CaF_2 + 33% CaO + 33% Al_2O_3 by weight.

Charpy, tensile and compact tension test pieces were cut from the ingots as shown in Fig. 2. Sufficient material for comprehensive fracture toughness and fatigue testing was available only from ingot 42. To obtain an adequate number of test pieces from the 70 mm diameter ingot, material from close to the ingot surface was utilized, but sufficient material was available close to the ingot centre-line for the larger-diameter ingots. Two test piece orientations were evaluated, namely longitudinal test pieces in which the general plane of fracture was normal to the macroscopic ingot growth direction, and transverse test pieces in which the fracture plane was parallel to the ingot growth direction (Fig. 2).

The mechanical properties of the top and bottom of each ingot were determined to take into account not only the variations in composition along an ingot length but also changes in solidification conditions arising from the presence of a water-cooled plate at the ingot base. For comparison purposes, transverse and longitudinal test pieces were also cut from a 100 mm diameter bar of vacuum-degassed wrought En25. All test pieces were given a heat treatment appropriate to gun barrel forgings before machining to final size, namely, austenitize at 850°, quench in oil, temper at 580°C, quench in oil reheat to 400°C and cool in air.

Charpy notch toughness tests were carried out at temperatures in the range -19°C to +80°C in accordance with the requirements of Australian Standard 1544, Part 2, 1975, while all tensile tests were conducted at room temperature (21°C) in accordance with the requirements of Australian Standard 1391, 1974. Fatigue tests were also performed at room temperature on a servohydraulic machine using a load ratio of 0.1 and fixed load limits to give an increasing stress intensity amplitude with crack growth. Cyclic loading followed a sinusoidal wave form and crack lengths were monitored

---

* Ingots of adequate quality for inclusion in the evaluation programme could not be produced with the d.c. electrode positive power mode. Electrode feed rate was difficult to control, resulting in the formation of ingots with extremely irregular surface finish.

automatically using a high sensitivity potential drop system [20]. Fatigue tests were terminated when crack length (a) reached 0.70 of the specimen width (W); the remaining uncracked ligament being still sufficient for a meaningful fracture-toughness determination [21]. The fracture toughness tests were made in accordance with ASTM E399. Where valid K_{IC} values were not obtained, because of insufficient specimen thickness and excessive plasticity during testing, the test records were re-analysed according to the J - estimation procedure proposed by ASTM [22], which allows a smaller specimen thickness. Values of J were converted to a stress intensity factor K_J, using the relationship $J=K^2/(1-\nu^2)E$ where ν is Poisson's ratio and E is Young's Modulus. A small uncertainty arose from the need to estimate the point of crack extension.

The composition of each ingot was determined at regular intervals along its length. As well, selected mechanical test pieces were analysed at positions immediately adjacent to fracture surfaces.

3. RESULTS

3.1 Compositional Changes

The composition of each ingot as well as that of the electrode from which it was formed and that of the wrought material used for the comparisons of mechanical properties are given in Table II. Only the composition of the extreme ends of each ingot are shown in this Table but these results reflect the extent of the variation in composition along an ingot length.

A substantial loss of the easily-oxidizable elements silicon and manganese was recorded for ingots 42 and 44, which were remelted in air. The chromium and titanium contents of ingot 44 were also significantly lower than those of the corresponding electrode material. While a considerable loss of silicon occurred during the remelting of ingot 43 (argon atmosphere), the overall composition of this ingot closely matched that of its electrode. The aluminium content of each ingot varied substantially and was generally much higher than that of the corresponding electrode. Maximum aluminium pick-up occurred in ingot 43 which was remelted using a slag containing 33 wt.% Al_2O_3.

The sulphur content of ingots 42 and 44 was about 20% below that of the corresponding electrode. A much higher degree of desulphurization, approximately 75%, was achieved in the bottom half of ingot 43 but this fell to about 30% in the top half.

3.2 Mechanical Properties

3.2.1 Tensile, Notch Impact and Fracture Toughness Tests

The tensile, notch impact toughness and fracture toughness results determined for the ESR ingots and the wrought En25 are listed in Tables III, IV and V, respectively. The values recorded for the wrought En25 were extremely sensitive to testing direction, with the longitudinal values being considerably higher than the transverse values. For about the same proof and ultimate strength levels, the longitudinal properties of the ESR ingots were also higher than their corresponding transverse properties, but only slightly so.

At the same sulphur level, the transverse and longitudinal tensile properties of the 100 mm diameter ESR ingots were higher than the transverse properties of a wrought En25 steel and, in some instances, approached the longitudinal properties of the material. The transverse and longitudinal impact toughness and fracture toughness values determined for the 100 mm diameter ingots approximated the transverse wrought results (Fig. 3 and Table V). The highest longitudinal and transverse as-cast tensile and impact results were recorded for the bottom half of ingot 43 (Tables III and IV and Fig. 4); the sulphur level of this material was half that of the wrought En25. The mechanical properties of the 70 mm diameter ingot tended to be substantially lower than those recorded for the larger ingots and, in some cases, were much less than the transverse wrought properties.

For the two ingots in which sulphur content was maintained constant along the full length (ingots 42 and 44), higher tensile and impact properties were generally recorded for the ingot top half (Fig. 5). The longitudinal impact toughness of ingot 44 did not conform to this pattern, slightly higher values being obtained for the bottom half of this ingot. Where the sulphur content varied along the ingot length, ingot 43, higher mechanical properties were recorded for the lower sulphur (bottom) half of the ingot (Fig. 6).

The various differences in the impact toughness of the cast and wrought material presented in Table IV and Figs. 3-6 were most pronounced in the upper shelf energy region. The transition temperatures of the as-cast ingots were similar to that of the wrought material tested in the transverse direction.

3.2.2 Fatigue Tests

Fatigue crack growth rates were determined for a range of stress intensities which are likely to be encountered by a gun barrel in service. They are plotted as log (da/dN) against log (ΔK) in Fig. 7 for the longitudinal test pieces and in Fig. 8 for the transverse test pieces. Here, da/dN is the rate of crack growth, and ΔK is the alternating stress intensity factor. Except for the extreme values of stress intensity, the data show a linear trend on the log-log plots. This linear portion is commonly associated with crack growth by ductile striation formation (Stage IIb regime in the spectrum of fatigue crack growth), and is interpreted using the Paris-Erdogan equation [23]

$$da/dN = C(\Delta K)^m$$

where C and m are material constants.

Although the longitudinal as-cast fatigue data were slightly displaced from the wrought data the separation is not significant. Similar "m" values of approximately 2.5 were recorded for both materials. The excellent duplication of the longitudinal as-cast data in Fig. 7 should be noted. The transverse wrought and as-cast data overlapped and, as well, coincided with the longitudinal data (Fig. 8). Again, the slopes were similar. This consistency implies that no effects of processing history or testing direction can be detected. Sufficient material was not available to enable the region of crack growth which involves a combination of striation formation and ductile overload to be examined in detail.

3.3 Inclusion Ratings

Evaluation of optical microscopy of samples taken from each ingot revealed that ingots 42, 44 and the top half of the ingot 43 contained numerous rounded as well as elongated manganese sulphide inclusions, and also duplex inclusions and clusters of angular inclusions. The angular inclusions and the darker phase in the duplex inclusions were bright in cross-polarized light indicating that they were probably aluminium oxides. This was subsequently confirmed by electron probe micro-analysis. Although the bottom half of ingot 43 contained fewer sulphides and duplex inclusions than the top half, the overall oxide content of ingot 43 appeared higher than that of the other ingots. Numerous oxide clusters were observed on the fracture surfaces of the mechanical test pieces cut from the top of ingot 43 (Fig. 9), whereas only isolated oxide clusters were visible on the fracture surfaces of the test pieces taken from the other ingots - see section 3.4 on fracture surface appearance.

The inclusion content of the three ingots could not be rated using conventional techniques, such as those described in ASTM E45-76, because they can only be applied to wrought material. Ingot samples were also examined by the Commonwealth Steel Company, and they advised that the inclusion level was much higher, particularly in regard to oxides, than that of the low-alloy ESR steels which they are producing [24]. The average 10 worst field rating for the wrought En25 material using ASTM E45-76 Method D was

A (sulphide type)	B (alumina type)	C (silicate type)	D (globular oxide type)
1.70H	1.20T	0	0.70T

where H(Heavy) and T(Thin) refer to inclusion thickness.

3.4 Fracture Surface Appearance

The most conspicuous difference in fracture appearance between the as-cast and the wrought test pieces was the presence on the fracture surfaces of the former of regions of intergranular fracture (Figs. 10-12). Frequently, these were distinctively dendritic in form (Fig. 13), particularly in the smaller diameter ingots.

3.4.1 Tensile and Notch Impact Test-Pieces

The extent of intergranular fracture varied with ingot size, with position along the length of an ingot, and with testing direction and temperature. Extensive areas of intergranular fracture were observed on the fracture surfaces of transverse test pieces cut from all three ingots, with those from ingot 44 displaying the greatest amount of this type of fracture and those from ingot 43 the least. Although intergranular fracture was most prevalent on the fracture surfaces of transverse test pieces, longitudinal test pieces cut from the top of ingot 44 also exhibited substantial regions of grain boundary fracture. Grain boundaries which had opened normal to the main fracture plane were occasionally observed on the fracture surfaces of longitudinal test pieces taken from ingots 42, 43 and the bottom of ingot 44 (Fig. 14). The transverse test pieces from the bottom of ingot 42 appeared to

be significantly more prone to intergranular fracture than those from the top half. For all ingots, grain boundary fracture during notch impact testing occurred over the entire range of test temperatures (-196°C to +80°C); the most extensive areas being formed during fracture at the higher test temperatures (Fig. 11).

Detailed examination of the intergranular regions using scanning electron microscopy revealed a variety of structures. Clusters of manganese sulphides (Type II sulphides) which have a fern-like appearance were common on the fracture surfaces of test pieces taken from ingot 44 (Fig. 15). At the higher test temperatures these ferns were surrounded by large areas of small microvoids (Fig. 15). The sulphides lying in the microvoids were typically 0.1-0.5 μm in diameter. At lower test temperatures approaching -196°, the microvoids were replaced by quasi-cleavage (Fig. 16).

Isolated ferns were seen on the fracture surfaces of the test-pieces taken from ingot 42. On some grain boundary regions of this ingot comparatively large sulphides which had grown parallel to the direction of grain growth were also observed (Fig. 17). The intergranular regions of the larger diameter ingots were covered almost entirely by microvoids containing small sulphides similar to those shown in Fig. 15. Microshrinkage was a common feature of the intergranular fracture areas of all ingots (Fig. 18).

The fracture mode in the transgranular regions varied through quasi-cleavage at very low test temperatures, a combined mode at intermediate test temperatures, to microvoid coalescence at high test temperatures. An unusual feature of the transgranular fracture regions in ingots 42 and 44 was the presence of numerous patches of microvoids which resembled craters in appearance (Fig. 19). The voids contained fine sulphide particles typically 0.1 μm in diameter. In the case of the Charpy test pieces these craters were detected over the entire range of test temperatures (Fig. 19).

In order to support these fracture observations, sections of test pieces from ingots were polished and then etched with the 10% HNO_3/10% [illegible] which is widely used to detect sulphide precipitation on grain boundaries and crystallographic planes. Evidence of extensive networks of sulphide precipitation on both sites was developed in ingots 42 and 44. Only [illegible] of grain boundary sulphide precipitation were detected in [illegible].

[illegible] Test Pieces

[illegible] fracture was observed on the fracture surface of the [illegible] test pieces taken from ingot 42, notably in the regions where [illegible], K_I, exceeded 40 $Mpam^{\frac{1}{2}}$ and where the test piece was [illegible] loading (Fig. 12). This mode of fracture was much more [illegible] fracture surface of the transverse test piece (Fig. 12). [illegible] occurred by ductile microvoid formation and coalescence, similar in appearance to that observed on the tensile and notch [illegible] surfaces.

[illegible] loading, crack extension in the transgranular regions [illegible] striation formation. This was the case for both the [illegible] test pieces. At the higher stress intensities the crack [illegible] branched and pockets of ductile overload were evident.

Here, comparatively large voids were frequently formed around sulphide inclusions which were roughly spherical in the as-cast material and elongated in the wrought material. Patches of small microvoids similar to those shown in Fig. 20 were also observed in the high stress intensity region of the transverse and longitudinal as-cast test pieces. Similar patches were also detected in those areas of the fracture surfaces of these test pieces formed during fracture toughness testing.

4. DISCUSSION

Substantial changes in composition which occurred during the remelting of two of the ingots may be attributed mainly to inadequate control over the oxygen potential of the slag bath. The loss of elements such as titanium, silicon, manganese and chromium clearly indicates that a high oxygen potential existed in the slag bath throughout remelting [27]. Retention of these elements was higher for the third ingot which was remelted under an argon atmosphere. However, some loss of silicon still occurred, possibly because this approach did not completely exclude oxygen from the furnace atmosphere. The aluminium-silicon transfer mechanism outlined in Equation 4 (see section 1.1.2) may have contributed substantially to this silicon loss as the ingot was remelted using a slag with a high alumina content. Supporting evidence for this proposal is the high aluminium levels in this ingot.

Significant differences between the composition of the consumable electrode and that of the remelting ingot has also been observed by the Commonwealth Steel Company. During the first few months of operation of their commercial ESR furnace, 1.5 tonne ingots were produced without the deliberate addition of deoxidants to the slag bath, in line with advice received from overseas. Substantial amounts of aluminium, silicon and manganese were lost to the slag, and the extent of these losses appears to have been exacerbated by a dry air system which continuously supplied oxygen to the furnace atmosphere.

The extent of desulphurization achieved in the present three ingots was influenced by slag basicity and furnace atmosphere as outlined in section 1.1.2. Although the slag used to produce ingots 42 and 44 nominally did not contain any basic oxides, the pyrohydrolysis effect (Equation 3) in combination with an air atmosphere in the mould cavity (Equation 2) has resulted in some sulphur removal. Whilst the use of a more basic slag for the remelting of ingot 43 caused much greater sulphur removal in the bottom half of this ingot, this high degree of desulphurization could not be maintained over the entire ingot length. Because of the low level of oxygen in the furnace atmosphere, desulphurization decreased as the sulphur content of the slag approached saturation level.

In spite of the loss of reactive elements such as silicon and manganese during remelting and the general pick-up of aluminium, the mechanical properties of the as-cast material overall compared favourably with those of the wrought material. From the point of view of process control, the most suitable as-cast material to compare with the wrought material was ingot 43. The chemical composition of this ingot was closest to that of the original electrode material and also to that of the wrought En25. This is undoubtedly why the mechanical properties of ingot 43 were the highest of the three ingots and also compared most favourably with those of the wrought material.

While the mechanical properties of the as-cast ingots did not exceed those of the wrought En25, they were much less anisotropic. Anisotropy is known to be due mainly to the elongation of inclusions during hot-working [29]. Elongated inclusions present a much greater surface area to a crack front when they lie in the plane of fracture than when they are aligned normal to it. It is significant to note that, for the notch impact test, the greatest degree of anisotropy in the wrought En25 was exhibited in the upper temperature region where the influence of inclusions on the fracture path is known to be most pronounced (Fig. 3). The as-cast ingots were not mechanically worked in any way and therefore did not display the same degree of anisotropy (Figs. 3, 5 and 6). However, the transverse as-cast properties were without exception lower than the longitudinal properties, largely because of the role that the grain boundaries played in the fracture process. In the transverse test pieces the grain boundaries were aligned roughly parallel to the fracture plane and the extensive amount of intergranular fracture which occurred clearly indicates that they provided the lowest energy fracture path, particularly when they contained numerous inclusions as was the case in ingots 42 and 44.

Difference in mechanical properties between ingots may be linked to the extent of intergranular fracture. For example, the mechanical properties of ingot 44 were the lowest of the three ingots and the fracture surfaces of the test pieces taken from this ingot displayed the greatest area of grain boundary fracture (Fig. 11). By contrast, maximum properties were obtained with ingot 43, in which intergranular fracture was minimal. Variations in properties along the length of ingots 42 and 44 may also be linked to the extent of grain boundary fracture. Ingot 43 is an exception in that sulphur content is an additional factor which must be considered. The superior performance of the lower sulphur end of this ingot clearly shows that sulphur level has an important influence on the mechanical properties of cast as well as wrought ESR steels.

Variations in the extent of intergranular fracture may be related to the structures observed in the grain boundary regions. The fracture path in, and therefore mechanical properties of, ingot 44 were controlled by the numerous elongated sulphides which precipitated in the interdendritic regions. The same effect was seen in ingot 42 but to a lesser degree. The extensive formation of these sulphides in the grain boundaries of ingot 44 may account for the more dendritic nature of the fracture surfaces. In most instances these sulphides displayed the classic fern-like appearance characteristic of Type II sulphides but there were occasions in ingot 42 where the directionality of their growth was closely linked to that of the dendrites. The type of sulphide which forms during the solidification of steel is known to be strongly influenced by the oxygen level in the steel [30,31]. Type II sulphides are reported to form at intermediate oxygen levels, i.e. at levels below that at which Type I sulphides form (>0.01 wt% oxygen) and above that of a fully-killed steel [31]. Mitchell [10] has found that the metal oxygen level during electroslag remelting may be high enough to precipitate Type II sulphides. That the Type II sulphides were most common in ingot 44 and absent from ingot 43 is additional evidence that significantly different slag oxygen potentials prevailed during the remelting of these ingots. The extent of sulphide fern formation is also affected by the amount of sulphur available, and it should be noted that the sulphur content of ingot 44 was the highest of the three ingots. It is well-documented that Type II sulphides deleteriously affect the mechanical properties of steel; the results obtained

for ingot 44 confirm that ESR steel in the as-cast condition is no exception. To obtain maximum performance from as-cast steel, it is recommended that an adequate deoxidation procedure be used during remelting and also that sulphur removal be a prime aim.

The other form of Grain boundary sulphide detected was small particles of α-MnS, roughly spherical in shape. These sulphides occurred in vast numbers and, during fracture, nucleated fine microvoids. The overall appearance of these fracture regions was characteristic of that caused by the solid-state precipitation of sulphides on austenitic grain boundaries after heating at temperatures high in the austenitic region [25]. This phenomenon is well-known in steel forgings, where it is frequently called overheating or grain boundary sulphide precipitation, the latter term being the one preferred [32]. This form of sulphide precipitation has only been observed on a few occasions in steel castings which have not been subjected to a high temperature heat-treatment after solidification. Two notable occurrences have been in an ingot produced by the vacuum arc remelting (VAR) process [33] and in small investment castings with a sulphur content similar to that of ingots 42 and 44 [34]. The cooling rates of ESR and VAR ingots are comparable. Furthermore, mechanical properties are most likely to be affected when grain boundary sulphide precipitation occurs at cooling rates in the range 10-400°C/min; the cooling rates of 70 and 100 mm diameter ESR ingots fall well within this range [16].

The mechanism proposed [34] to account for grain boundary sulphide precipitation in castings is similar to that which is now well-documented for steels subjected to high temperature heat-treatments. At the completion of solidification, the austenite may contain an appreciable amount of sulphur in solid-solution. On further cooling, solubility decreases and the sulphur is precipitated as small α-MnS particles on the austenitic grain boundaries existing at the time. The findings of the present work support this model. Susceptibility to precipitation of this nature is reported [34] to be increased in steels containing more than 2.0% nickel and less than 1.0% manganese, the amounts of these elements in the ESR ingots being 2.2% and 0.5%, respectively. Thus, the chemical composition and thermal history of the ESR ingots, particularly ingots 42 and 44, appear to have increased their sensitivity to grain boundary sulphide precipitation during the initial cooling after solidification.

Precipitation of α-MnS particles on crystallographic planes has not previously been recorded for cast steels, although it has been observed in material which has been reheated before mechanical working [37]. As with precipitation on grain boundaries, similar conditions are undoubtedly necessary for precipitation on planes in wrought and cast steels, i.e., coarse grain size, and therefore long diffusion distances, as well as supersaturation of sulphur within the bodies of the grains after solidification or reheating [25]. Although the αMnS particles on the planes and boundaries of the austenitic grains may provide the lowest energy fracture path, a high energy fracture process is involved nevertheless [38].

Solidification geometry is also believed to have influenced the extent of intergranular fracture. Establishment of a liquid metal pool of reasonable size is difficult near the base of small diameter ESR ingots because of the rapid heat removal through the base-plate and mould wall. As a result, the pool profile in this region is normally flat and the growth direction strongly axial [39]. Thus, the fracture plane of the longitudinal and transverse test

pieces taken from the lower portion of each ingot, particularly the 70 mm diameter ingot, was aligned either normal to, or parallel to, the grain boundaries. Consequently, fracture surfaces displayed either a large component of intergranular crack propagation (transverse test pieces from ingots 42 and 44) or none at all (longitudinal test pieces from these ingots). Further along an ingot length where the influence of base-plate cooling is reduced, the pool deepens and the growth pattern becomes more radial. Alignment of grain boundaries with test piece orientation was therefore not as clearly defined in the top half of ingots 42 and 44 and this was reflected in less intergranular fracture in the transverse test pieces. Furthermore, the evidence of this form of fracture in longitudinal test pieces increased, notably in those from the smaller diameter ingot.

The change in solidification geometry along the length of ingot 43 was not as pronounced as in the other two ingots, possibly because it was shorter and the melt rate was slower (Table I). The lower sulphur content of the bottom half of this ingot also may have offset the greater propensity for intergranular fracture observed in this region of the other ingots. It is possible that the mechanical properties of the top half of ingot 43 may have been higher than those of the bottom half if the sulphur content had been uniform along the ingot length.

5. SUMMARY

1. The three ingots of low-alloy steel were produced in an experimental ESR furnace.

2. Significant losses of elements such as titanium, silicon, manganese and chromium which occurred during the remelting of two of these ingots were associated with inadequate control over the oxygen potential of the slag bath.

3. The composition of the third ingot which was remelted under an inert atmosphere using a more basic slag was similar to that of the electrode material. Substantial desulphurization occurred in the bottom half of this ingot.

4. The tensile, notch impact toughness, fracture toughness and fatigue properties of these ingots in the as-cast, heat-treated condition approximated those determined for wrought electric furnace steel of similar composition tested in the transverse direction. The mechancial properties of the as-cast material were much less anisotropic than those of the wrought En25.

5. The highest tensile and notch impact properties for as-cast material were recorded for the low sulphur end of the ingot remelted under an argon atmosphere, indicating the important effect that sulphur level has on the performance of as-cast ESR steel. The properties of this material approached those determined for the wrought En25 tested in the longitudinal direction.

6. Extensive areas of intergranular fracture were observed on the fracture surfaces of the mechanical test pieces cut from the ESR ingots, particularly the transverse test pieces. This mode of fracture was associated with the presence at the high temperature austenitic grain boundaries of Type II sulphides and small α-MnS particles. Grain boundary sulphide precipitation

during the initial cooling of cast steel occurs by a similar mechanism to that established for wrought steel.

6. ACKNOWLEDGEMENTS

The authors wish to thank Mrs. V. Silva and the staff of the Photographic Section for their assistance with the fractography.

7. REFERENCES

1. Duckworth, W.E. and Hoyle, G. (1969). "Electroslag Refining", Chapman and Hall Ltd., London, p.7, 20, 29, 56.

2. "Electroslag Remelting and Plasma Arc Melting", National Materials Advisory Board, National Academy of Sciences, Washington, D.C. 1976, p.7.

3. Andrew, R.C. and Weston, G.M. (1978). "The Electroslag-Refining Process", Metals Australasia, 10, May/June, p.6.

4. Holzgruber, W. (1974). Proceedings Fifth International Symposium on Electroslag and Other Special Melting Techniques, Carnegie-Mellon Institute of Research, Penn., Oct., Part I, p.70.

5. Wagner, H.J. and Bar Avi, K. (1979). Metals Technology, 6, p.420.

6. Lowe, E.M. and Hogg, A. (1973). "Application of ESR to Alloy-Steel Forgings", Proceedings of a Conference on Electroslag Refining, University of Sheffield, January, p.68.

7. Liddle, J.F. (1973). "Removal of Inclusions During Electroslag Refining", Chemical Metallurgy of Iron and Steel, Iron and Steel Institute, p.66.

8. Lloyd, G.W., Owen, I.A. and Baker, L.A. (1971). J. Aust. Inst. of Metals, 16, 1, p.17.

9. Allibert, M., Wadier J.F. and Mitchell, A, (1978). Iron Making and Steel-making, 5, No. 5, p.211.

10. Mitchell, A. (1976). "The Electroslag Remelting of HY130 Steel", Metallurgy Department, University of British Columbia, April.

11. Paton, B.E., Medovar, B.I. and Boiko, G.A. "Outlook for Electroslag Casting", Proceedings of the Fifth International Symposium on Electroslag and Other Special Melting Technologies Carnegie-Mellon Institute of Research, Penn., p.239.

12. Mitchell, A. and Akhtar, A. (1977). "Electroslag Castings - A Potential Substitute for Forgings", Symposium on the Effects of Melting and Processing Variables on the Mechanical Properties of Steel", Winter Annual Meeting of ASME, Atlanta, Georgia, November-December, 1977.

13. Mitchell, A. (1978). Modern Casting, 68, November p.86.

14. Klein, H.J., Venal, W.V. and Love, K.L. (1976). "Production of Electroslag Remelted Hollow Ingots" Stellite R & D Report 9045.

15. Venal, W.V., Gross, R.T., Klein, H.J. and Colangelo V.J. (1977). Electric Furnace Proceedings, __, p.264.

16. Irving, R.I., (1978). Iron Age, October 9, p.43.

17. Gulya, J.A. and Wilson, A.D. (1979). "Electroslag Remelted Material For Use in the As-Cast and Heat-Treated Condition", to be presented at the 1979 Winter Annual Meeting of ASME, New York City.

18. Underwood, J.H. (1978). Expt. Mechs., 18, 9, p.350.

19 Andrew, R.C., Weston G.M. and Hughes P.C., (1978). "Metals Australasia, 10, July, p.18.

20. Clark, G. (1979). "A High Sensitivity P.D. Technique for Fatigue Crack Growth Measurements", MRL Report 755.

21. Knott, J.F. (1973). "Fundamentals of Fracture Mechanics", Chapter 5, London (Butterworths).

22. ASTM Recommended Procedure for J_IC Determination, Minutes of Committee E24-01-09, 3 January, 1977.

23. Paris, P. and Erdogan, F. (1963). Trans. ASME 85, p.528.

24. Porcheron, R. Commonwealth Steel Company, Private Communication.

25. Andrew, R.C., Weston, G.W. and Southin, R.T. (1976). J. Aust. Inst. of Metals, 21, June-September, p.127.

26. Hoyle, G. British Steel Corporation, Private Communication.

27. Nafziger, R.H. (1976). "Thermochemistry of the Electroslag Process", The Electroslag Melting Process, Bureau of Mines Bulletin 669, p.26.

28. Ormerod, G. Commonwealth Steel Company, Private Communication.

29. Baker, T.J. and Charles, J.A. (1971). "Influence of Deformed Inclusions on the Short Transverse Ductility of Hot Rolled Steel", Conference on the Effect of Second Phase Particles on the Mechanical Properties of Steel, Scarborough, p.79.

30. Wells, R.G. (1974). "Metallographic Techniques in the Identification of Sulfide Inclusions in Steel", Proceedings of a Conference on Sulfide Inclusions in Steel, New York, American Society for Metals, p.123.

31. Baker, T.J. "Use of Scanning Electron Microscopy in Studying Sulfide Morphology on Fracture Surfaces", Ibid., p.135.

32. Andrew, R.C. and Weston, G.M. (1980). "Nomenclature for High Temperature Phenomena in Low Alloy Steels", Metals Australasia, 12, (3), p.7.

33. Barker, T.J. and Johnson R. (1973). JISI, 211, November, p.783.

34. Barker, T.J. and Harrison, W.D. (1975). Metals Technology, 2, May, p.201.

35. Glue, D.R., Jones, C.H. and Lloyd, H.K.M. (1975). Ibid., 2, September, p.416.

36. "A Guide to the Solidification of Steel", Jernkontoret, Stockholm, 1977, p.11.

37. Andrew, R.C. and Weston G.M. (1977). Metal Science, 11, April, p.142.

38 Joy, G.D. and Nutting, J. (1971). Proc. ISI/BISRA Conference, "Effect of Second-Phase Particles on Mechanical Properties of Steel", Scarborough, p.95.

39. Andrew, R.C. and Weston, G.M. Unpublished work.

TABLE I

CONDITIONS FOR INGOT PRODUCTION

Melt Details	Ingot 42	Ingot 43	Ingot 44
Nominal Slag Composition*	90F/0/0/10/0	33F/33/0/33/0	90F/0/0/10/0
Slag Mass, g	1300	1600	900
Nominal Ingot Dia., mm	100	100	70
Ingot Length, mm	480	380	525
Electrode Dia., mm	63	63	44
Current, amps	1350-1460	1330	900
Voltage, volts	20-22	20	24
Melt Rate kg/h	46	37	25
Power Mode	d.c.-ve	d.c.-ve	d.c.-ve
Atmosphere	Air	Argon	Air

* The slag compositions are listed in accordance with a system of slag rotation devised by ESRT [1]. The weight per cent of calcium fluoride is given first, suffixed by an F. The weight per cent of oxides is then given in the order lime, magnesia, alumina and silica.

T A B L E II

CHEMICAL COMPOSITION OF ELECTRODES AND INGOTS IN WT%

Ingot Number	Position*	C	Si	Mn	P	S	Ni	Cr	Mo	V	Al	Ti	Cu
42	E	0.32	0.19	0.56	0.020	0.026	2.2	0.72	0.54	<0.01	0.026	ND	0.10
	T	0.32	0.12	0.49	0.019	0.022	2.3	0.71	0.48	<0.01	0.005	ND	0.11
	B	0.31	0.06	0.37	0.020	0.020	2.1	0.67	0.48	<0.01	0.088	ND	0.10
43	E	0.34	0.16	0.55	0.020	0.027	2.2	0.71	0.47	<0.01	0.024	ND	0.11
	T	0.34	0.09	0.50	0.019	0.019	2.2	0.70	0.49	<0.01	0.15	ND	0.11
	B	0.34	0.05	0.53	0.021	0.006	2.1	0.70	0.47	<0.01	0.063	ND	0.11
44	E	0.30	0.18	0.58	0.020	0.031	2.4	0.65	0.47	0.05	0.014	0.02	0.12
	T	0.29	0.08	0.39	0.020	0.025	2.0	0.56	0.45	<0.01	0.073	<0.01	0.11
	B	0.30	0.08	0.41	0.019	0.028	2.1	0.50	0.44	<0.01	0.035	<0.01	0.28
Wrought En25 for Comparison of Mech. Props.		0.40	0.24	0.61	0.015	0.020	2.4	0.60	0.47	<0.01	0.03	0.02	0.09

* E - electrode remelted to produce ingot. T - 25 mm from top of ingot. B - 25 mm from base of ingot.

TABLE III

TENSILE RESULTS

Test Piece Location	Sulphur Content*, wt%	Longitudinal Results					Transverse Results				
		0.2% Proof Stress, MPa	Tensile Strength MPa	% Elong.	Reduction in Area, %	Fracture Strength, MPa	0.2% Proof Stress MPa	Tensile Strength MPa	% Elong.	Reduction in Area, %	Fracture Strength, MPa
Top Ingot 42	0.020	1080	1170	15	49	1720	1070	1170	12	35	1560
		1070	1170	15	47	1720	1070	1170	11	30	1480
Bottom Ingot 42	0.020	1050	1140	10	31	1500	1050	1140	9	23	1380
		1050	1140	13	38	1560	1060	1140	9	22	1369
Top Ingot 43	0.019	1090	1170	13	44	1660	1090	1170	11	37	1580
		1090	1170	14	50	1760	1090	1180	9	23	1380
Bottom Ingot 43	0.010	1090	1190	13	48	1760	1070	1160	13	41	1620
		1100	1190	12	46	1700	1080	1170	13	43	1640
Top Ingot 44	0.024	1080	1150	12	34	1480	1080	1160	10	26	1420
		1080	1150	15	49	1700	1070	1150	8	21	1380
Bottom Ingot 44	0.024	1040	1130	11	38	1580	1020	1110	7	15	1200
		1030	1120	14	31	1300	1040	1130	7	11	1220
Wrought En25	0.020	1120	1200	16	58	1940	1070	1150	7	20	1360
		1120	1200	16	58	1920	1060	1140	8	22	1380

* The sulphur content of test pieces taken from the top and bottom of each ingot was measured.

TABLE IV

RESULTS OF CHARPY TEST PERFORMED AT TEMPERATURES IN THE RANGE -196°C TO +80°C

Test piece Location	Nominal Diameter, mm	Sulphur Content*, wt%	Notch Impact Toughness at °C, Joules														
			Longitudinal Results									Transverse Results					
			-196	-150	-120	-80	-50	-30	0	20	80	-196	-120	-80	-30	20	80
Top Ingot 42	100	0.020	5	5	10	14		23	26	29	27	5	9	10	16	22	22
Bottom Ingot 42	100	0.020	7	11	12	16		22		22	22	4	7	8	12	18	16
Top Ingot 43	100	0.019	7		15	25 25		26		31	34	4	15	18	19	25	30
Bottom Ingot 43	100	0.010	5 8	15	18	22		37		42	44	5	15	16	27	29	31
Top Ingot 44	70	0.024	6		10	13 14		15		19	18	4	8	7	11	12	12
Bottom Ingot 44	70	0.024	-		14	18		20		22	22	4	4	5	10	8	10
Wrought En25	120	0.020	18	22	27	43.5 44	60	71 72	65	61	54	5 5	9.5	12	18	18	22

* The sulphur content of test pieces taken from the top and bottom of each ingot was measured.

T A B L E V

FRACTURE-TOUGHNESS TEST RESULTS

Sample	Sulphur Content wt%	Test Direction	K_Q MPam$^{\frac{1}{2}}$	Overall Validity	$K_{I_{c_{\frac{1}{2}}}}$ MPam$^{\frac{1}{2}}$	K_J MPam$^{\frac{1}{2}}$
Ingot 42	0.02	Trans.	101	yes	101	
		Long.	109	yes	109	
		Long.	116	no		122
Wrought En25	0.02	Trans.	107	yes	107	
		Long.	154	no		197
		Long.	154	no		182

Specimen width 50.8 mm, thickness 25.4 mm in all cases.

0.2% proof stress (by) values in Table III used in validity calculations.

All tests performed at room temperature (+21^{o}C).

Fatigue starter crack profiles met ASTM validity criterion in all cases.

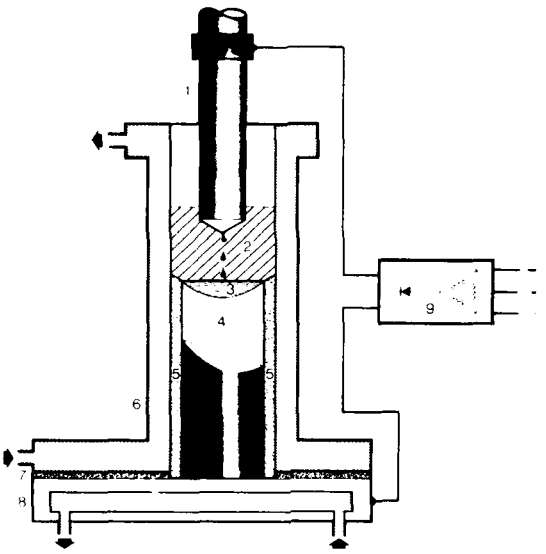

FIG. 1 - Schematic representation of the electroslag-refining process

1. Consumable electrode
2. Molten slag bath
3. Pool of molten metal
4. Solidified ingot
5. Solidified slag skin
6. Water-cooled mould
7. Electrical insulation
8. Water-cooled base-plate
9. Power supply

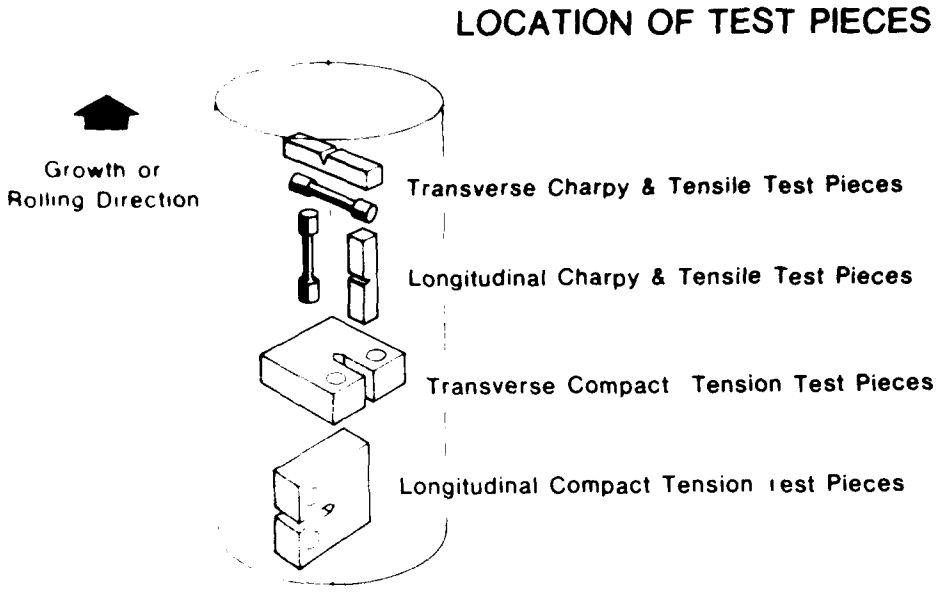

FIG. 2 - Schematic diagram showing location of test pieces. The longitudinal axis represents both the macroscopic growth direction of the ESR ingot and the working direction of the wrought bar of En25.

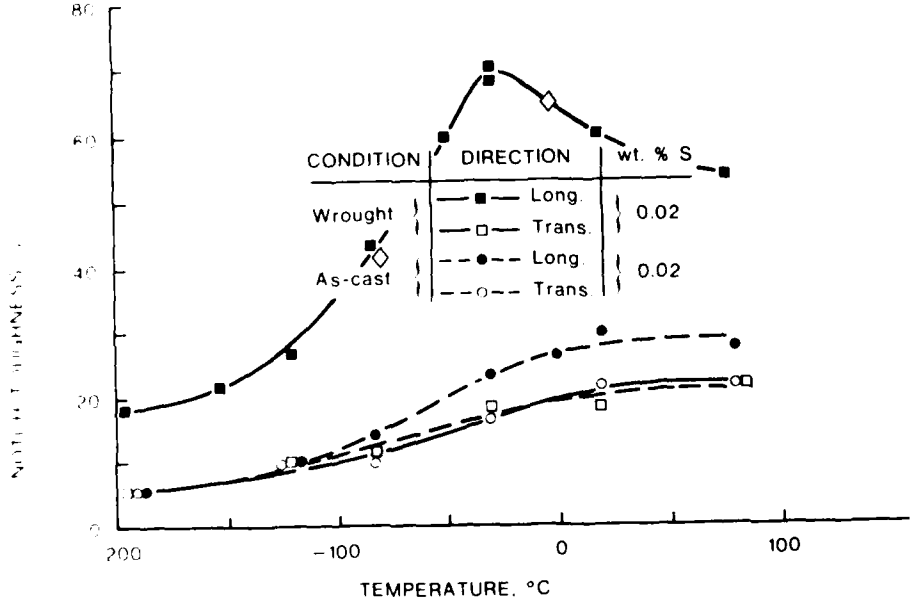

FIG. 3 - Comparison of the longitudinal and transverse notch impact toughness of a 100 mm diameter ESR ingot and wrought En25 of similar sulphur content.

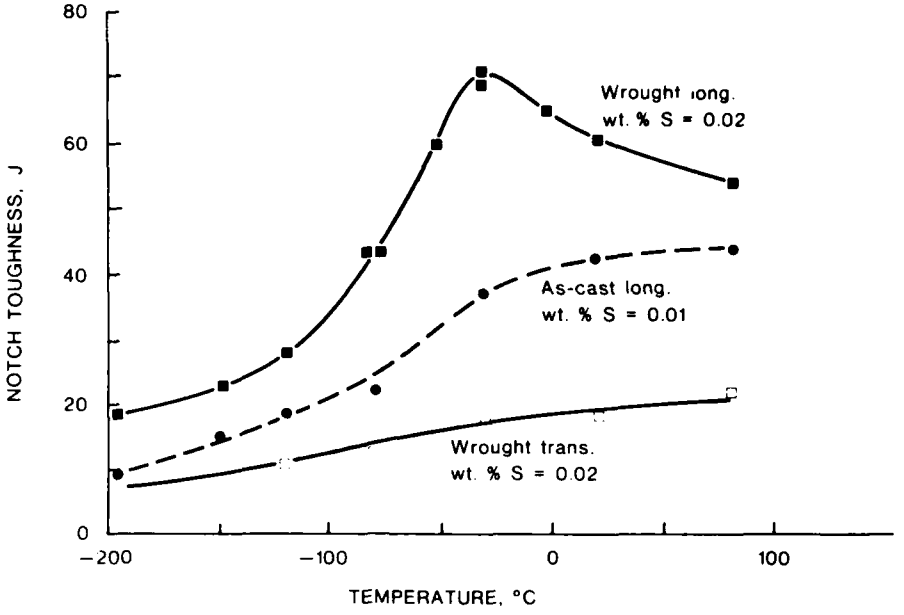

FIG. 4 - Comparison of the longitudinal notch impact toughness of ingot 43 with that of wrought En25 bar.

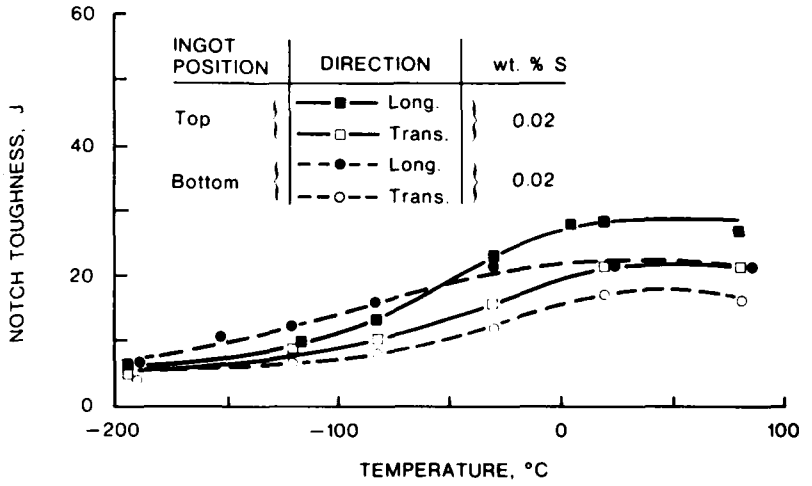

FIG. 5 - Comparison of the longitudinal and transverse notch impact toughness of the two halves of ESR ingot 42.

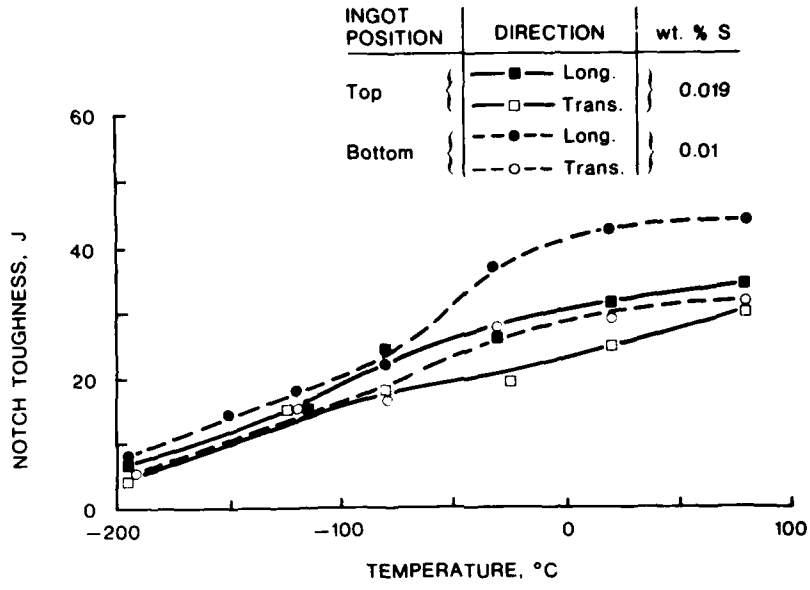

FIG. 6 - Comparison of the longitudinal and transverse notch impact toughness of the two halves of ESR ingot 43.

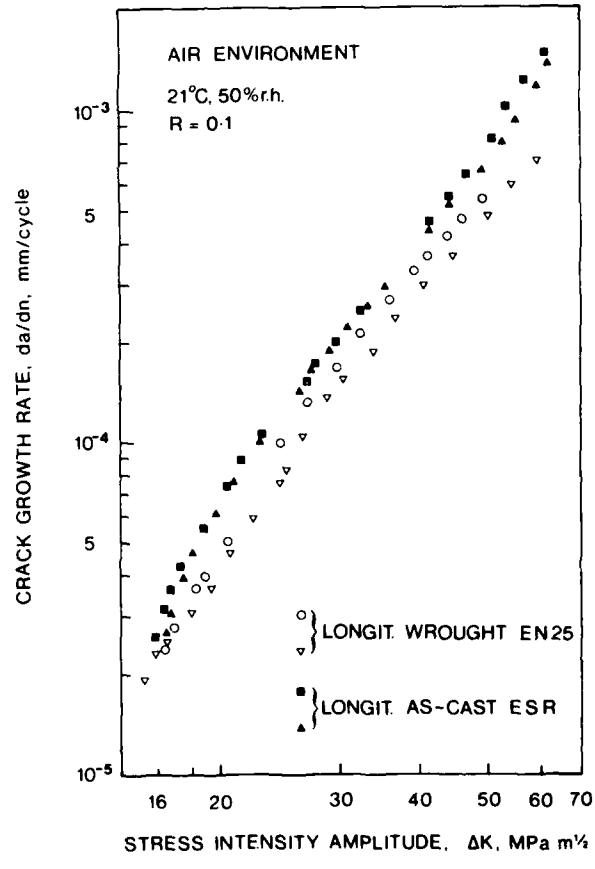

FIG. 7 - Comparison of the fatigue crack growth rates as a function of stress intensity for longitudinal wrought En25 and as-cast ESR test pieces of similar sulphur content.

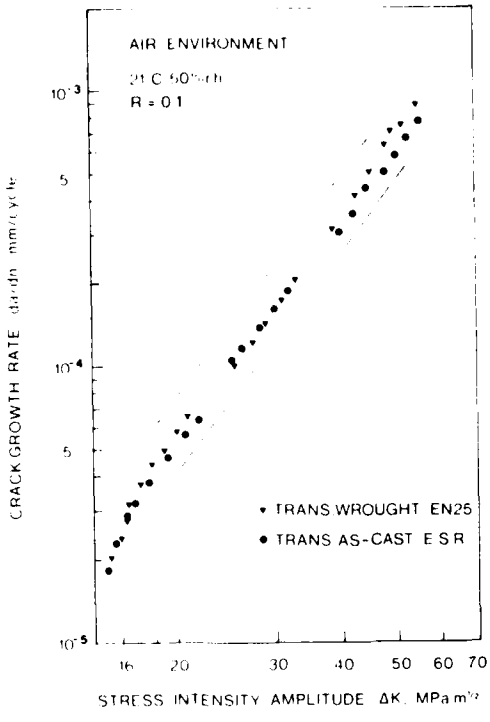

FIG. 8 - Comparison of fatigue crack growth rates as a function of stress intensities for transverse wrought En25 and as-cast ESR test pieces of similar sulphur content. The spread of the corresponding longitudinal data is indicated by the dotted lines.

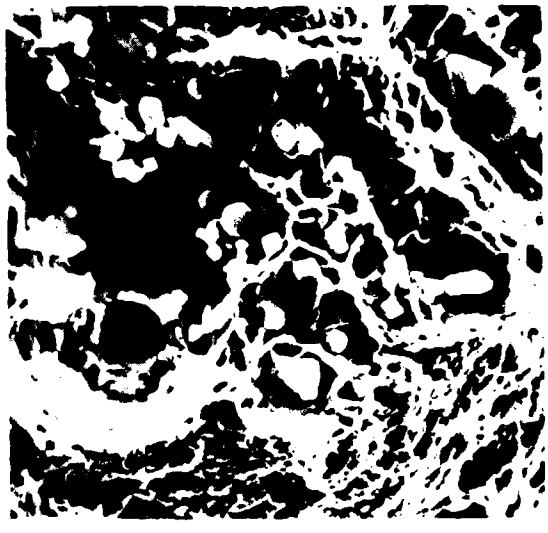

FIG. 9 - Cluster of oxide inclusions on the fracture surface of a mechanical test piece cut from ingot 43. X1680

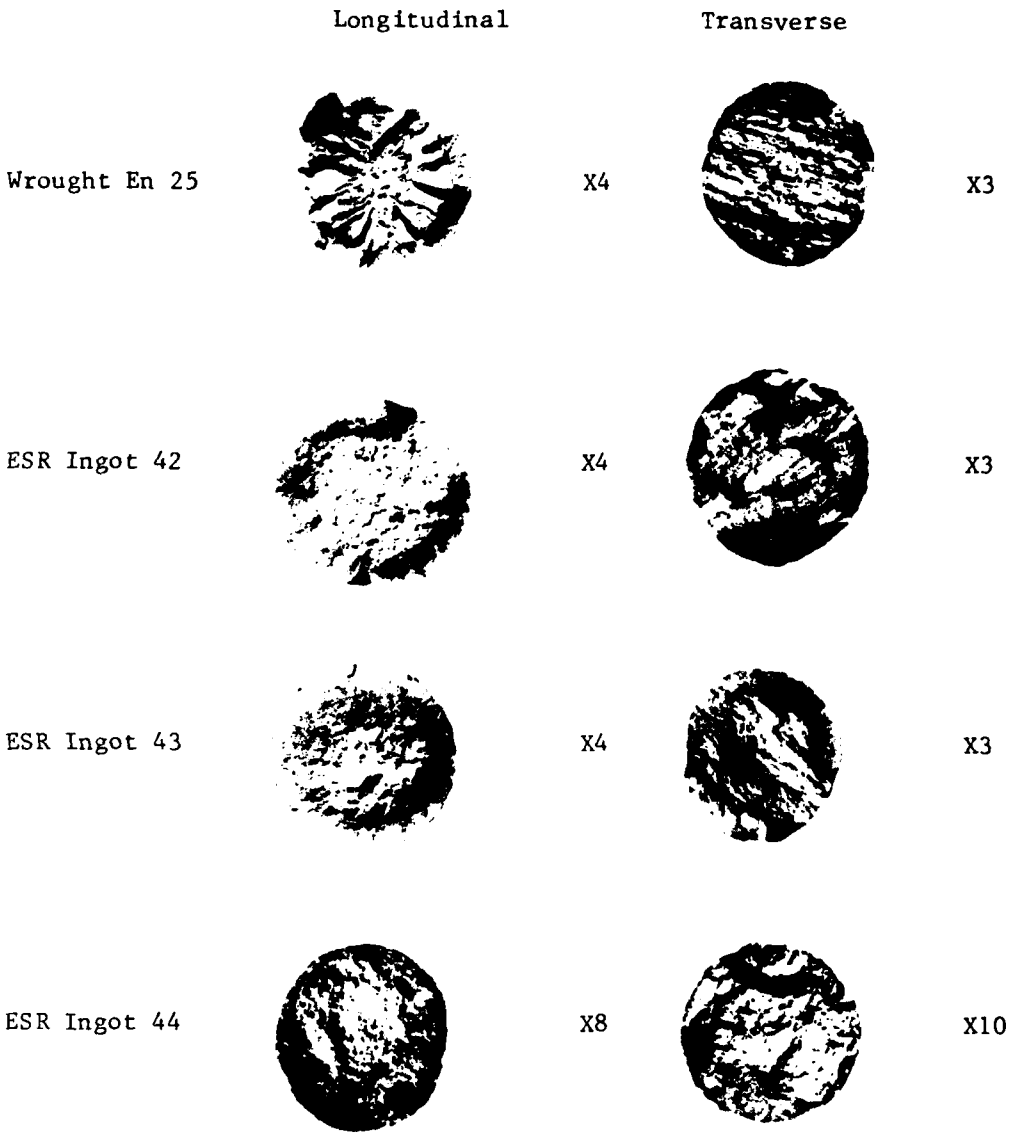

FIG. 10 - Fracture surface appearance of tensile test pieces.

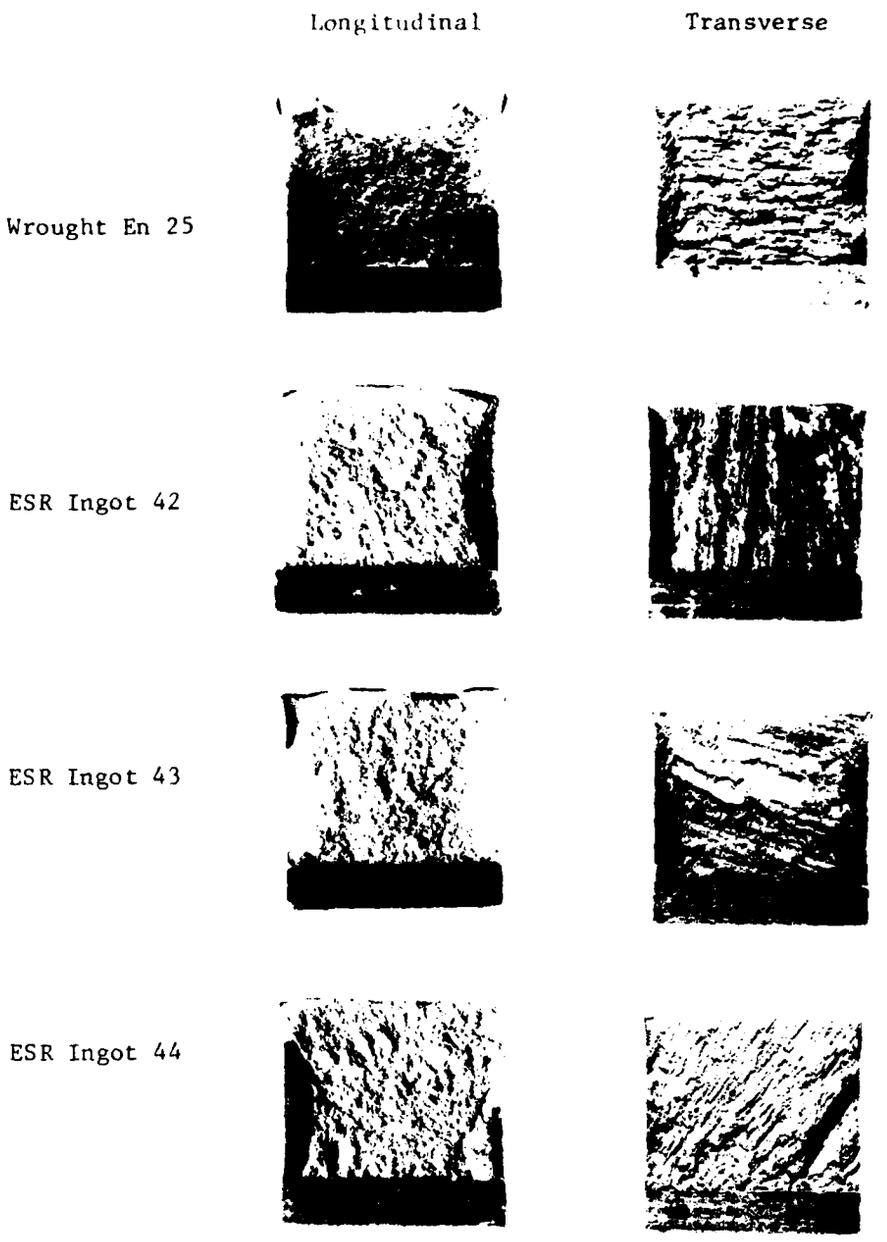

FIG. 11(a) - Fracture appearance of Charpy test pieces. X3
Test temperature + 80°C

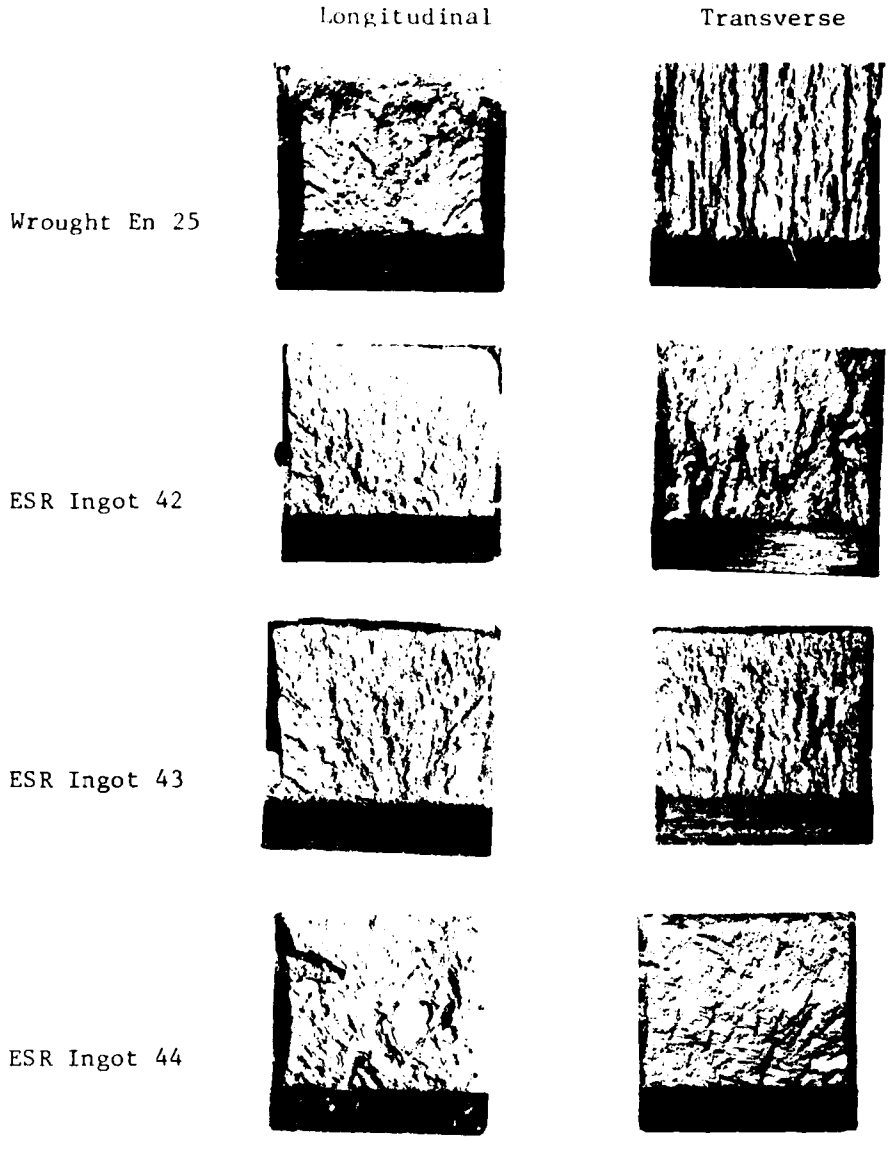

FIG. 11(b) - Fracture appearance of Charpy test pieces. X3
Test temperature - 120°C.

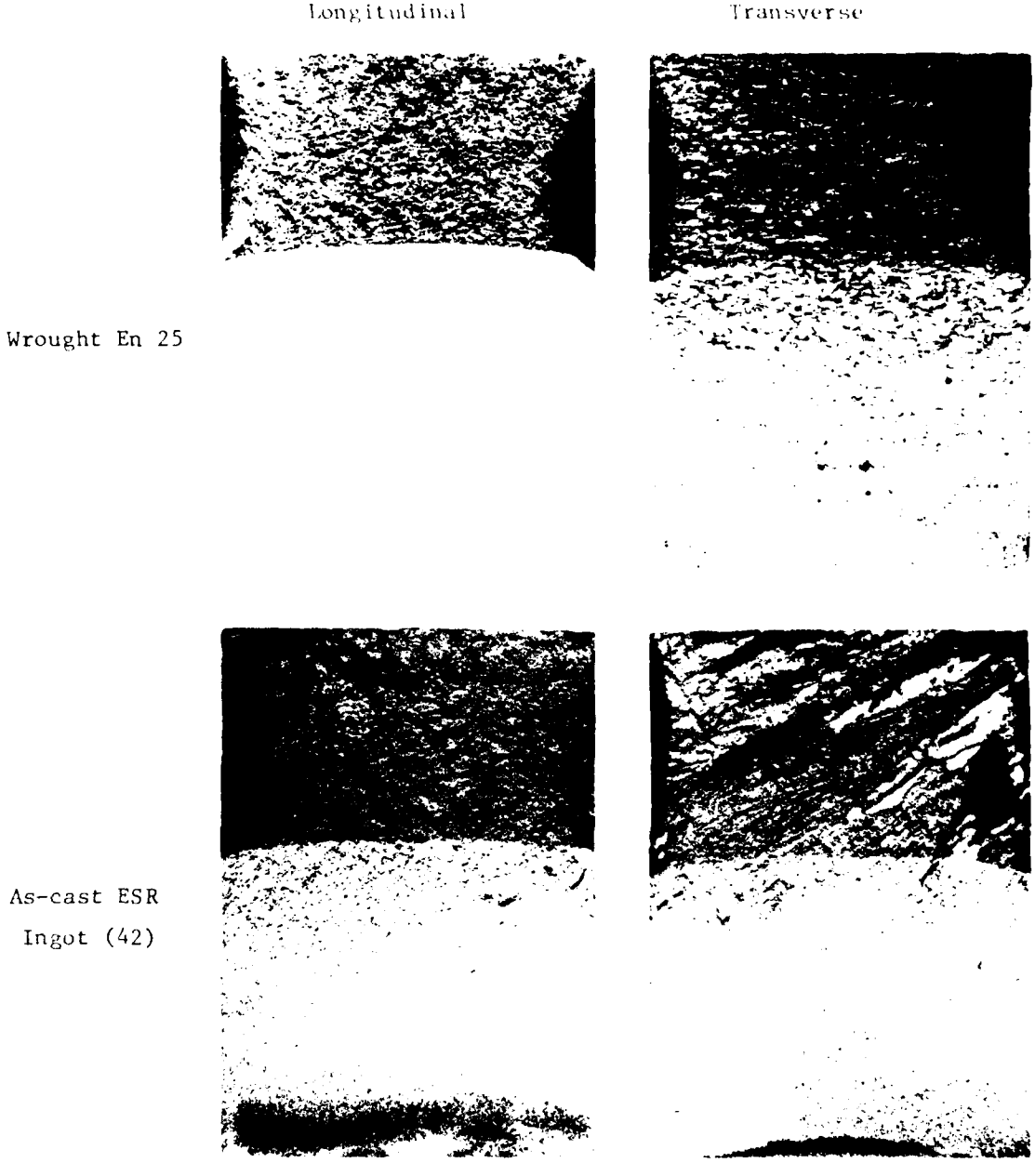

FIG. 12 - Fracture appearance of compact-tension test pieces. In each case the fatigue crack has extended upwards over $\sim \frac{2}{3}$ of the field, the bowed crack front is contrasted against the darker region of overload fracture. All X2.

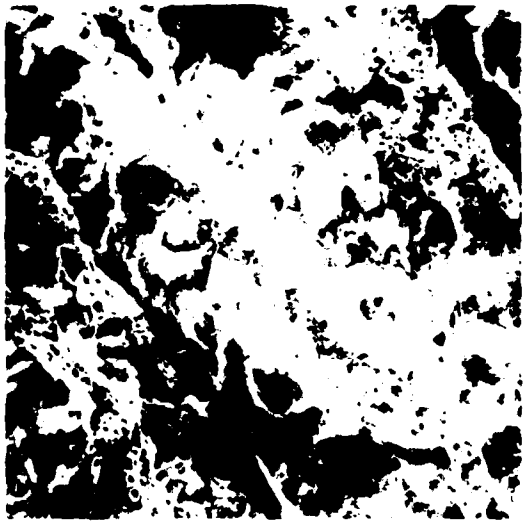

FIG. 13 - Extensive area of intergranular fracture on the fracture surface of a transverse notch impact test piece from ingot 44. X80.

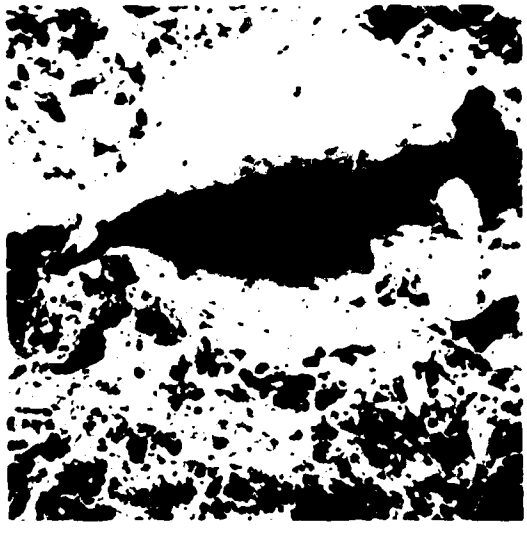

FIG. 14 - Grain boundary fracture normal to the main fracture plane. Longitudinal notch impact toughness test piece. X85.

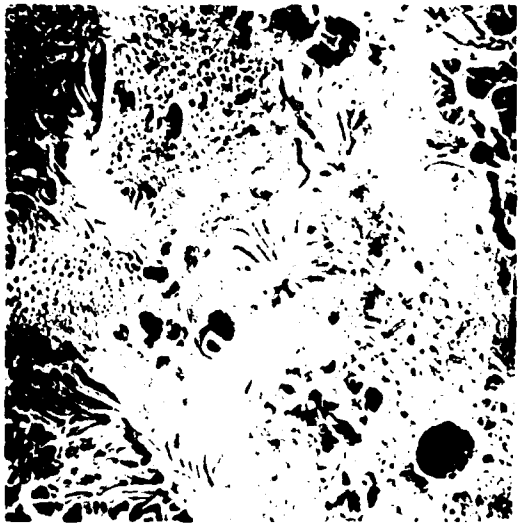

(a)

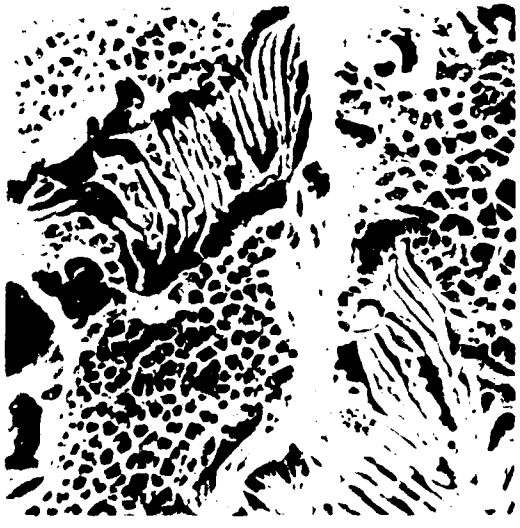

(b)

Two examples of intergranular fracture in a notch impact test piece from inset of Type II manganese sulphides surrounded by extensive areas of fine microvoid coalescence. The sulphides which nucleated the microvoids formed by solid-state precipitation during the initial cooling of the ingot.

(a) [illegible] (b) [illegible]

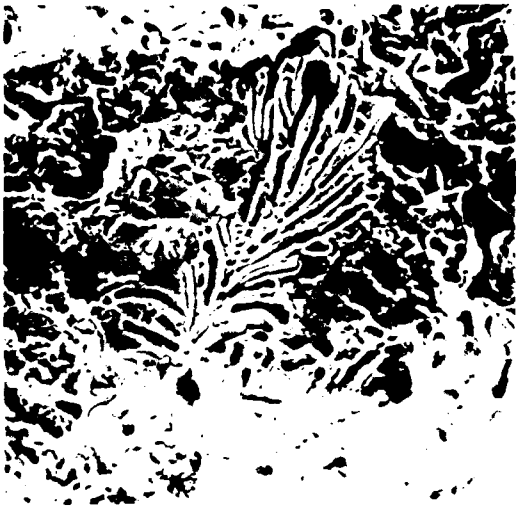

FIG. 16 - Intergranular fracture in a notch impact test piece from ingot 44. Manganese sulphide ferns surrounded by areas of quasi-cleavage. Test temperature - 196°C.

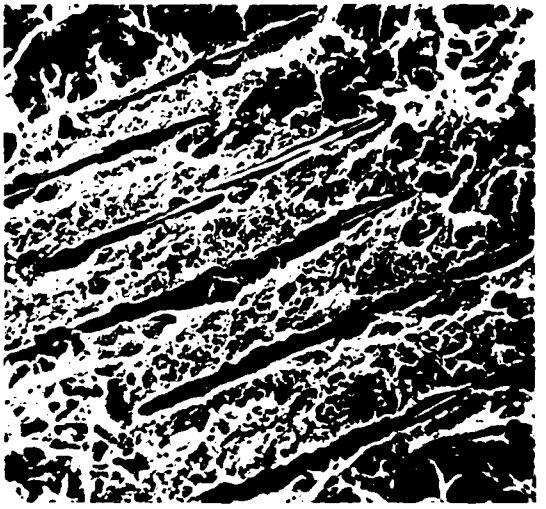

FIG. 17 - Directional growth of sulphides on some intergranular fracture regions of a notch impact test piece from ingot 42.

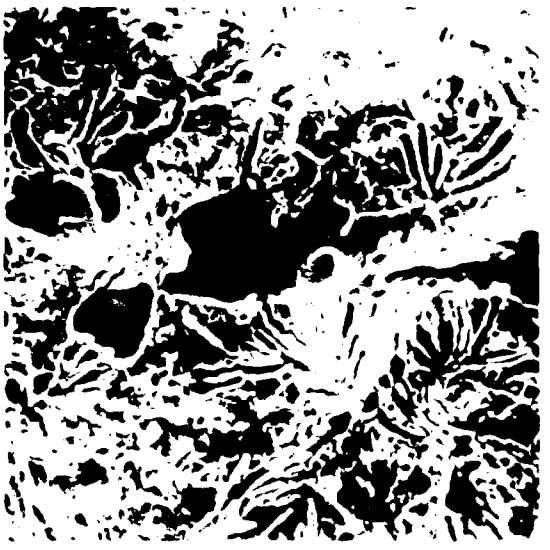

Region of intergranular fracture in a notch impact test piece from ingot 44. Test 3 microshrinkage and manganese sulphide ferns. ×200.

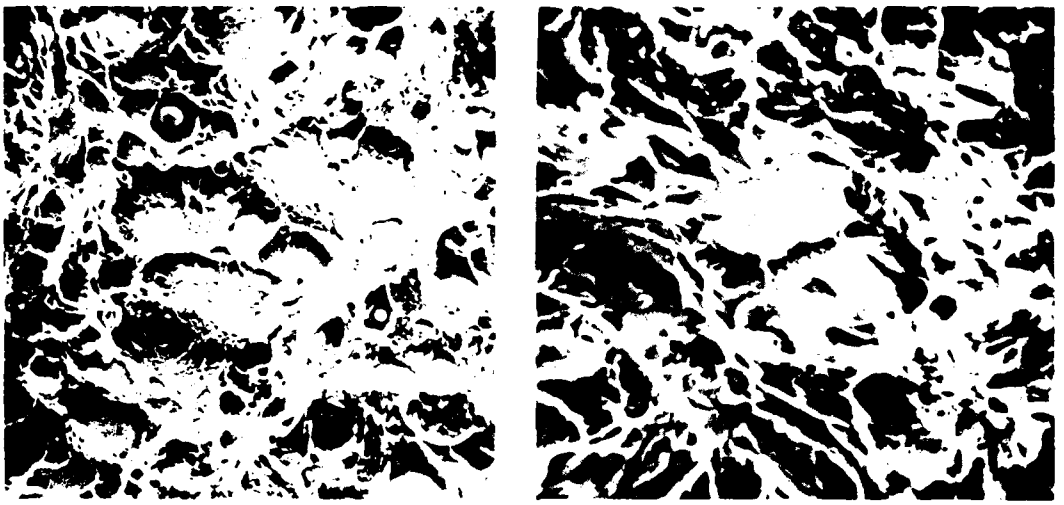

(a) (b)

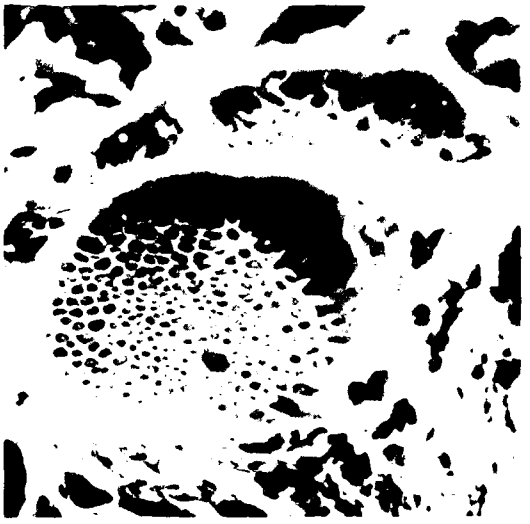

(c)

Fig. 19 - Cratered facet formation in regions of transgranular fracture after testing at various temperatures.

(a) -80°C X800

(b) -196°C X100

(c) Detail of cratered facets, the sulphides [illegible] X8000

(MRL-R-786)

DISTRIBUTION LIST

MATERIALS RESEARCH LABORATORIES

Chief Superintendent
Superintendent, Metallurgy Division
Dr J.C. Ritter
Dr R.C. Andrew
Mr G.M. Weston
Dr G. Clark
Library
Librarian, Materials Testing Laboratories, NSW Branch
(Through Officer-in-Charge)

DEPARTMENT OF DEFENCE

Chief Defence Scientist
Deputy Chief Defence Scientist
Controller, Projects and Analytical Studies
Controller, Service Laboratories and Trials
Army Scientific Adviser
Air Force Scientific Adviser
Naval Scientific Adviser
Chief Superintendent, Aeronautical Research Laboratories
Chief Superintendent, Weapons Systems Research Laboratory,
Defence Research Centre
Chief Superintendent, Electronics Research Laboratory,
Defence Research Centre
Chief Superintendent, Advanced Engineering Laboratory,
Defence Research Centre
Superintendent, Trials Resources Laboratory, Defence
Research Centre
Senior Librarian, Defence Research Centre
Librarian, RAN Research Laboratory
Officer-in-Charge, Document Exchange Centre (17 copies)
Technical Reports Centre, Defence Central Library
Central Office, Directorate of Quality Assurance - Air Force
Deputy Director Scientific and Technical Intelligence,
Joint Intelligence Organisation
Head, Engineering Development Establishment
Librarian, Bridges Library, Royal Military College

DEPARTMENT OF PRODUCTIVITY

NASA Canberra Office
Head of Staff, British Defence Research and Supply Staff (Aust.)

DISTRIBUTION LIST

(continued)

OTHER FEDERAL AND STATE DEPARTMENTS AND INSTRUMENTALITIES

The Chief Librarian, Central Library, CSIRO
Australian Atomic Energy Commission Research Establishment

MISCELLANEOUS - OVERSEAS

Defence Scientific and Technical Representative, Australian High Commission, London, England
Assistant Director/Armour and Materials, Military Vehicles and Engineering Establishment, Surrey, England
Reports Centre, Directorate of Materials Aviation, Kent, England
Library - Exchange Desk, E01 Administration Building, National Bureau of Standards, Washington, USA
US Army Standardization Representative, C/o DGAD (NSO), Canberra
The Director, Defence Scientific Information and Documentation Centre, Delhi, India
Colonel B.C. Joshi, Military, Naval and Air Adviser, High Commission of India, Red Hill, ACT
Director, Defence Research Centre, Ministry of Defence, Kuala Lumpur, Malaysia
Exchange Section, British Library, Lending Division, Yorkshire, England
Periodicals Recording Section, Science Reference Library, The British Library, Holborn Branch, London, England
Library, Chemical Abstracts Service, Ohio, USA
INSPEC: Acquisition Section, Institution of Electrical Engineers, Herts, England
Overseas Reports Section, Defence Research Information Centre, Ministry of Defence, Kent, England
Engineering Societies Library, New York USA